Modeling the Integration of Flow, Cell and Microcarrier Biomechanics in a Stirred Tank Bioreactor

Proof-of-Concept Report v1.0 - *The CMMC, July 2020*

1. Motivation

Increasing worldwide demand for meat is driving the growth of environmentally detrimental factory farming. Cultivated meat is a potentially more sustainable alternative to factory farming that could mitigate water contamination, land use, and disease spread. As a nascent technology, however, a number of challenges must be overcome before cultivated meat is available worldwide. Arguably the most fundamental challenge is the efficient production of biomass at scale.

At present, two significant issues stand in the way of scaling up production. First is the cost of media fed into the bioreactor to support cell growth. Media costs will decline as serum-free media technologies - already in use by some cultivated meat producers - eliminate the need for expensive serum and other animal-derived components. Further cost reductions are expected as media formulations transition from small quantities and custom combinations used in R&D to the higher volumes and more predictable demand typical of ingredients used in mass production. How much media cost reduction will be achieved through economy of scale though is a subject of debate.

The second impediment to scaling production is the efficacy of the bioreactor equipment itself at high production volumes. Cells require a nutritious, oxygen rich, homogeneous environment. At the same time cells consume some molecules such as cytokines and chemokines in the environment and excrete others. In live animals, vasculature delivers and collects molecules to sustain every cell's environment. In bioreactors, mixing the fluid acts as a coarse surrogate for vasculature. As bioreactor volume and cell density increases, maintaining a well-mixed environment tends to require faster fluid flow. A faster fluid flow can induce strong shear forces that cause cells to cease proliferating or to die.

Maintaining a favorable molecular environment for cells without subjecting them to excessive shear stress will require innovation in, and optimization of, bioreactor designs and processes. Both innovation and optimization require extensive experimentation. However, building physical prototypes and running experiments are slow and expensive. Virtual prototyping and experimentation through computer simulation promises to accelerate and lower the cost of progress. However, virtual experiments replicating actual bioreactor and biological behaviors are not immediate: we need first to develop predictive models of the bioreactor environment.

Tha main challenge in developing a predictive model of cells growing in a bioreactor is the complexity of the bioreactor environment and cell behavior. Media flow dynamics, forces, and mixing of media components need to be incorporated into the model. Simultaneously, cells growing on microcarriers, consuming nutrients, excreting waste, proliferating and dying introduces an additional layer of complexity. Thus, modeling the resulting system requires an altogether new multiscale methodology accounting for phenomena happening at diverse spatial and temporal scales.

2. The CMMC

In 2019 the Cultivated Meat Modeling Consortium convened as an interdisciplinary effort inviting integration of expertise in the diverse areas relevant to modeling cultivated meat production processes. This community is globally distributed with participants ranging from academic, commercial, industrial, philanthropic, and non-governmental organizations and individuals. Members represent expertise in relevant technologies, domains, and stakeholder populations, including biology, physics, and computer science, consumer products, and food science. Within the CMMC, teams convene to tackle challenges in collaboration with industry and academia.

One of these teams has convened around the challenge of developing computational models of cells growing in bioreactors to support the optimization of current bioprocesses, experimenting with new ones, and prototyping novel bioreactor designs *in silico.*

The current “Proof of Concept” (POC) project recapitulates experimental results reported in the literature for a simple stirred tank bioreactor. The POC illustrates the efficacy of the CMMC approach and the application of a new modeling methodology on cultivated meat production processes. Conversations around these tangible results serve to align the CMMC with industry partners around a shared understanding of current bioreactor processes and limitations. The POC also represents the beginning of a “branching tree” of possible avenues for exploring the application of modeling and computer simulations to optimize cultivated meat biomass and tissue generation. The POC began early in 2020 and is described in this report. However, several more years will be required to mature and apply this technology to state-of-the-art bioreactors.

3. Background on bioreactors

Bioreactors are manufactured systems designed to carry out aerobic or anaerobic biological processes in a controlled environment, and these systems can accommodate microorganism or cell-cultures for applications with either suspended or immobilized cells [1]. These devices span a huge size range from miniaturized setups that can be inoculated with a single cell [2] up to much larger units, such as the 2000 m^3 airlift loop reactor developed by Imperial Chemical Industries [3]. Across this size range, bioreactors are utilized in the food and beverage, pharmaceutical, chemical and environmental remediation industries, where the processes broadly focus on production of biomass, metabolite synthesis or biotransformation [1].

3.1. Bioreactor Diversity

To fulfill diverse applications across many industries, bioreactors come in different configurations and designs, which are partially influenced by cell type (suspension or adherent)

[4].Typically, bioreactor processes may be configured as batch, fed-batch or continuous setups, and designs pertinent to cultivated meat production can be broadly grouped as agitated or perfusion systems [5]. In the case of agitated bioreactors, this classification includes stirred tank systems, rotating wall bioreactors and rocking/wave bioreactors [6].

Stirred tank bioreactors are impeller-driven systems which are generally well-mixed and relatively homogenous in terms of nutrient and gas dispersion [7]. These ubiquitous reactors, widely used in pharmaceutical applications, have characteristic height-to-diameter ratios for cell culture applications, and can utilize different impeller designs to achieve either axial or radial flow [7]. Key performance considerations with stirred tank bioreactors include the power input, mixing time, and mass transfer and oxygen transfer coefficients, where gradients and spatial heterogeneities become more pronounced at larger vessel sizes [7]. Adherent cells can be grown in stirred tank systems with microcarriers, but this does render the cells more sensitive to agitation damage by shear forces and small intense eddies [8].

Turbulent flows and shear forces can induce cell damage, so configurations that produce fewer of these forces are of interest. Rocking bioreactors are designed to produce excellent mixing and gas transfer, but with reduced shear stress [6]. Furthermore, rocking bioreactors are simpler than the stirred bioreactors due to the absence of a sparger. Rocking (wave) bioreactors have also been shown to be very suitable for the cultivation of cells on microcarriers [9], and are under consideration for cultivated meat production [6].

The other broad class of bioreactors relevant to cultivated meat are perfusion systems which include packed-bed, fluidized-bed and hollow-fiber set ups [5]. With these designs, overall volumetric productivities are typically higher than agitated systems cells [10]. Cell immobilization also protects cells against shear forces and environmental stresses and is more representative of *in vivo* growth conditions, but immobilization does limit mass transfer of both substrates and products [6], [10].

3.2. Bioreactor Challenges

There are numerous challenges that must be addressed in growing cultivated meat biomass. One considerable challenge is that there are currently no commercial cultivated meat bioreactors or bioprocesses in existence. Generally, processes must be designed to achieve many rounds of replication as well as highly efficient and controlled differentiation and tissue maturation [5]. Numerous novel bioreactor designs are also likely needed given the diversity of animal protein categories and products [6]. Low cost media formulations of non-animal origin (serum-free) will be a further necessity for production scale cultivated meat bioreactors, and these require development.

Another input for cultivated meat, the starter (stem) cells, can be sensitive to turbulent flow and shear forces that induce cell damage and untimely differentiation [4]. Therefore, cultivated meat bioreactors must accommodate shear sensitivities while still achieving sufficient mass transfer,

oxygen transfer and adequate CO_2 removal [5], [10]. A suite of novel process analytical technologies specifically for cultivated meat bioreactors may also be required to track numerous parameters (e.g. biomass production and metabolite release) in real-time to optimize production, and later develop quality assurance practices for full-scale manufacturing systems [10].

Perhaps the predominant challenge in applying bioreactors to cultivated meat is the volume of biomass that must be created. Cultivated meat bioreactor designs have parallels in cell therapy and vaccine production bioprocesses, but these designs must be distinctive because of the vast number of cells that must be produced to create food instead of therapeutics [5]. Depending on the process particulars, a scale-up (industrial scale, commercial plants) or scale out (small scale, supplying regions) strategy may be appropriate, but mass production must be achieved either way. Process sustainability is another challenge for cultivated meat bioreactors, given the goal of displacing conventional animal protein. Here, highly efficient conversion of inputs into biomass must be achieved, which likely includes spent media recycling and waste valorization [5].

3.3. How Modeling Can Help

Given the research, design, process optimization and scaling challenges that lie ahead for cultivated meat bioreactor development, tools are needed to realize commercial manufacturing systems sooner. Computational modeling and simulation can help to address, and at least partially overcome, many of these challenges [6]. For one, computational simulation can be a far cheaper and faster alternative to performing physical experiments. Computational models can also help researchers pinpoint system interactions that matter, and guide researchers to identify those parameters that should be changed in later design.

Additionally, computational models allow researchers to make predictions under unobserved conditions as well as derive novel insights into phenomena not necessarily captured with real-time data acquisition. These include bioreactor gradient formation and heterogeneities, and cell-scale resolution into system behaviour. Computational models can be further harnessed to understand biological, physio-mechanical and fluid dynamic aspects of the bioreactor system in conjunction.

Foundational computational models should also be widely applicable across bioreactor designs. Once a base model is established, it can be easily extended to other bioreactor systems and allow for iterative refinement at far lower cost than redesigning and testing a physical bioreactor. Computational models can also predict how the system will behave in the future, and should be a more affordable and less time-consuming alternative to building out large-scale prototypes. In this way, modelling techniques can be developed to mirror experiments at high fidelity, and

should help physical experiments realize maximal efficiencies. All these qualities should allow cultivated meat bioreactors to come into existence sooner and achieve faster scaling.

Prior work using computer modeling and simulation to predict bioreactor behavior for numerous designs and configurations is summarized in [6].

4. Problem Statement

In any new endeavour “starting simple” has merit, as the principle promises high return in learning relative to investment of effort. Similarly, testing a new methodology on well-studied systems provides reliable feedback on its efficacy. Confidence in the methodology emerges from its consistently accurate predictions. In general, stirred tank reactors are very well-studied, and the simplest version is the stir-rod bioreactor without any control systems. With this in mind, the authors turned to an older research paper by Croughan *et al.*, [8] which provides both empirical and theoretical analyses of hydrodynamic effects on microcarrier cultures of FS-4 cells in a stir-rod bioreactor. In particular, the paper reports distinct trends for the influence of stir speed on biomass accumulation, and thus, growth rate.

The microcarrier cultures were grown in a simple bioreactor set-up that was agitated but was not aerated and had no pH control technology (Figure 1). A cylindrical rod suspended from above, immersed to two-thirds the depth of the liquid, and rotated at a constant speed agitates the fluid. Rotational speed was the only parameter varied in the experiments reported by Croughan *et al*. This and other parameters of the bioreactor system are specified in Table S1 of the supplemental material. In our model, we needed additional quantities not provided by Croughan *et al*, attributed below to other sources.

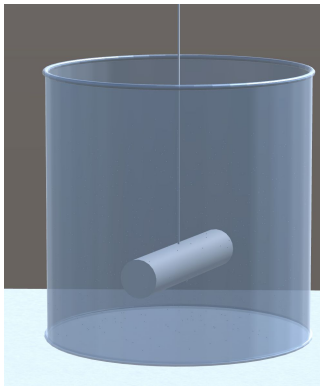

Figure 1. Bioreactor geometry

Croughan *et al*. studied how growth rate changes as a function of excessive agitation speed. Prior experimental results had established roughly 60 rpm to be a rate sufficient to provide the

needed supplies of nutrients and oxygen while higher rates reduced productivity. Croughan *et al.* were focused on rates of 60 rpm and above. They proposed an analytical model in which growth and death rates are exponential over time, resulting in population graphs that are piecewise linear when on a log-scale as shown in Figure 2. In their model, the growth (proliferation) rate exponent of cells is assumed constant throughout all experiments and the death rate is assumed to change with agitation speed. The rates are calculated based on these assumptions to best-fit data sampled from experiments.

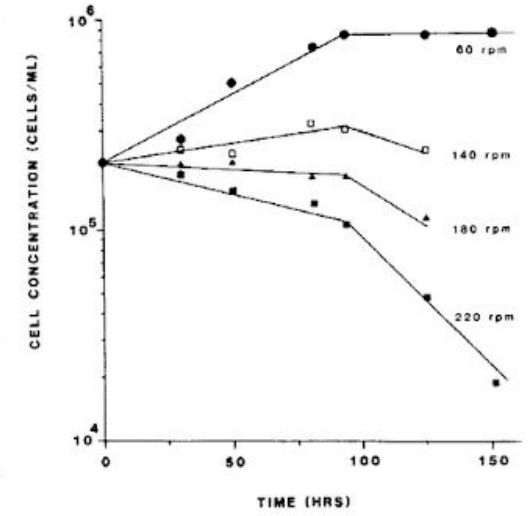

Figure 2. Growth of FS-4 cells on microcarriers at various stirring speeds. All cultures contained 3 g/L Cytodex 1 microcarriers and were in identical 250 ml vessels.

5. Approach

5.1. Methodology

The current aim of predicting cell growth as a function of rotor speed requires at very least connecting rotor speed to fluid flow and fluid flow to cell biology. Computational fluid dynamics (CFD) has been used for decades to model fluid flow in bioreactors and agent-based modeling (ABM) to model multicellular biology. We begin by summarizing these two widely-used and independent modeling methodologies. In addition, we describe how we integrate the two methodologies to create a new modeling approach.

5.1.1. Computational Fluid Dynamics (CFD)

CFD is a branch of three integrated disciplines of fluid mechanics, mathematics, and computer science. Along with two other basic approaches of experimental fluid dynamics and analytical fluid dynamics, CFD is one basic approach that uses numerical analysis and data structures to

analyze and solve fluid flow problems. CFD has been used in many engineering disciplines, including aerospace, automotive, biomedical, chemical, civil and environmental engineering.

In cultivated meat production, CFD can be used to simulate and understand the fluid flows in the bioreactors. The fluid flow in bioreactors is governed by three fundamental physical principles: 1) mass conservation, 2) F = ma (Newton's second law), and 3) energy conservation. These fundamental principles along with the constitutive laws relating the stress tensor in fluid to the rate of deformation tensor, are expressed in the form of partial differential equations, called Navier–Stokes equations.

In addition to the fluid flow in bioreactors, the nutrient distribution and movement inside bioreactors also can be simulated by incorporating the mass transport of particular chemical species with the CFD models. Though not modeled in the present work, we plan to exploit this capability in the future.

5.1.2. Agent-Based Modeling (ABM)

ABM generally represents a system by a collection of individual objects (the agents), each with a potentially unique behavior, as a function of interactions with each other and with their environment. A typical objective of ABM is to predict outcomes that emerge from these interactions as a function of the environment. An example application is traffic modeling in which each object is an automobile or a street light, the environment is the streets, and the emergent outcome is the total time spent stuck at traffic lights.

In biological applications, the ABM objects are often the cells themselves, each following rules that determine the conditions under which the cell, for example, grows, moves, adheres, divides, differentiates and dies as a function of the biochemical and physical environment. In the case of bioreactors, microcarriers can also be represented as agents and the emergent outcome of interest is often the overall rate of proliferation as a function of time and bioreactor properties.

5.1.3. Why integrate ABM with CFD?

While CFD has been used for decades to model fluid flow in bioreactors and ABM to model multicellular systems, neither one alone adequately answers the questions raised by scientists and engineers tasked with achieving the cost reductions necessary for cultivated meat to be cost-competitive with butchered meat products. Examples of these questions have arisen in our discussions with cultivated meat companies on the front-lines of development and cover a lot of ground:

Tank and rotor: What rotor and tank geometries result in fluid flow that maintains adequate mixing to deliver nutrients and oxygen to all cells while minimizing the stress on these cells that causes them to differentiate, quiesce or die?

Microcarriers: Microcarriers need not be spherical. What size, shape and density of microcarriers would similarly optimize conditions for growth?

Bioprocess: Changing rotor speed, adding additional microcarriers, adjusting oxygen and nutrient influx are some of the bioprocess parameters that can be modulated over time. What schedule optimizes conditions for growth?

Scale: Large bioreactors reduce cost due to economy of scale, yet physical experimentation is cost-prohibitive. How can all of the above be optimized for large-capacity bioreactors?

In all four areas of study, predicting how the fluid flow environment impacts cell biology and how cell biomass in turn affects fluid properties, over time, is invaluable if not prerequisite to performing the corresponding optimizations. By integrating CFD with ABM, we can capture the knowledge needed to make these predictions.

Combining these platforms in a more comprehensive model can generate novel insights and identify emergent properties in the system under study. Indeed, CFD and ABM have been used together in several diverse multiscale models that simulate disaster responses [11], cell and particle migration through blood vessels [12]–[15] and movement of zooplankton in complex flow environments [16].

Notably, CFD and ABM per se have never been used together to understand the process dynamics within a bioreactor relevant to cultivated meat. However, combined models for biological and physicochemical dynamics have been used to examine different parallel-plate bioreactor configurations for growth of tissue [17]. Here, a unilineage model was employed to describe the replication and differentiation of stem cells, and the physicochemical processes were modeled by the Navier-Stokes and convective-diffusion equations.

Next we examine in greater depth our approaches to CFD, ABM and their integration specific to modeling the current aim.

5.2. Computational Fluid Dynamics Model

The CFD model was developed in the commercial finite element method (FEM)-based simulation package COMSOL multiphysics. The CFD model includes five components: (1) geometry, (2) governing equations and their (3) boundary conditions, (4) mesh scheme, and (5) post-processing.

The CFD simulations of the bioreactor hydrodynamics are performed using COMSOL Multiphysics 5.5 for single phase flow (water liquid, ρ=998.2 kgm−3, μ=0.001003 Pa·s) and two rotation speeds N=60 rpm and 240 rpm. The turbulence model used is the standard k-ε model implemented in COMSOL, where k represents the turbulent kinetic energy, and ε represents the

dissipation of turbulent kinetic energy. A steady-state fluid flow was simulated using the following equations:

$$\rho(\boldsymbol{u}\cdot\nabla)\boldsymbol{u} = \nabla\cdot[-p\boldsymbol{I}+\boldsymbol{K}]+\boldsymbol{F}$$

$$\rho\nabla\cdot\boldsymbol{u} = 0$$

$$\boldsymbol{K} = (\mu+\mu_T)(\nabla\boldsymbol{u}+(\nabla\boldsymbol{u})^T)$$

$$\rho(\boldsymbol{u}\cdot\nabla)k = \nabla\cdot\left[\left(\mu+\frac{\mu_T}{\sigma_k}\right)\nabla k\right]+P_k-\rho\epsilon$$

$$\rho(\boldsymbol{u}\cdot\nabla)\epsilon = \nabla\cdot\left[\left(\mu+\frac{\mu_T}{\sigma_\epsilon}\right)\nabla\epsilon\right]+C_{\epsilon1}\frac{\epsilon}{k}P_k-C_{\epsilon2}\rho\frac{\epsilon^2}{k},\ \ \epsilon = ep$$

$$\mu_T = \rho C_\mu\frac{k^2}{\epsilon}$$

$$P_k = \mu_T[\nabla\boldsymbol{u}:(\nabla\boldsymbol{u}+(\nabla\boldsymbol{u})^T)]$$

where u is velocity, F is force, ρ is density, μ is viscosity.

In order to simulate the rotation of a rod impeller, the moving mesh technique is used, and the geometry is divided into three zones: (1) a cylindrical zone (imaginary domain for mixing) around (2) the rod impeller which rotates at the impeller speed and (3) a zone covering the rest of the vessel which is stationary, as shown in Figure 3.

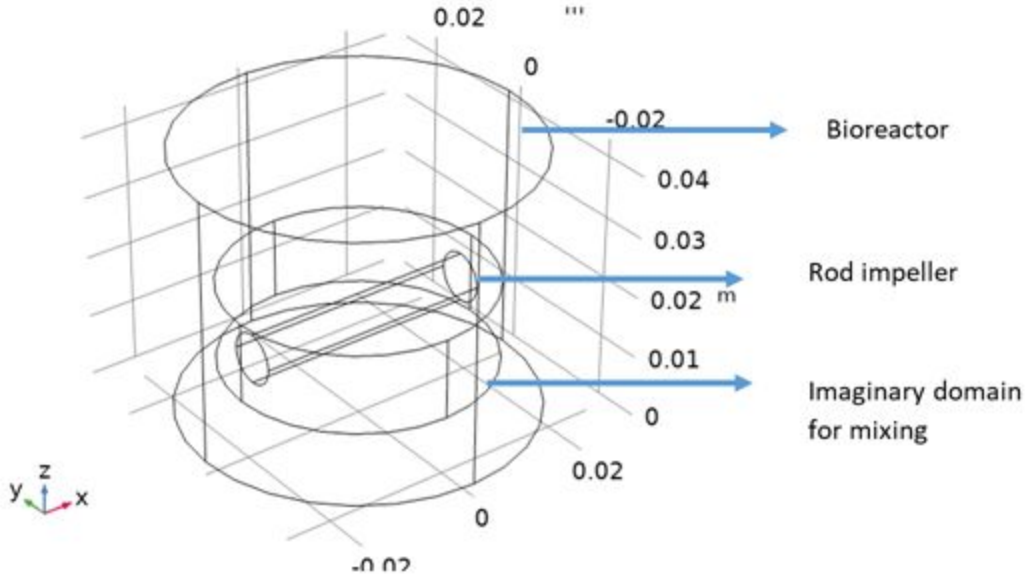

Figure 3. Geometry of the bioreactor with a rod impeller.

The geometry domain for the bioreactor is discretized into tetrahedral shaped elements forming a mesh. A total of ~1.7 million elements were generated. Once the simulation converges, the mesh nodes including their positions and corresponding velocities are exported as a data file.

From this fluid velocity data, the agent-based modeling platform can estimate the forces acting on cells and microcarriers that in turn influence their mechanical behavior and biological response. In the future, if desired, the spatial concentrations of environmental molecules injected into the system could also be modeled, simulated and exported to further inform the modeled biological response of cells.

5.3. Agent-Based Model

We developed a three dimensional agent-based model of cells growing on microcarriers moving in the fluid media of the stirred tank. In the ABM formulation, each cell and microcarrier is represented as a spherical agent that is propelled by forces calculated from the computed velocity field and the viscosity of the fluid media. By including the cells and microcarriers explicitly, the model allows us to study the relationships between mechanical interactions and important biological processes such as cell proliferation and cell death.

5.3.1. Equations of motion

We use Newton's equations to model the dynamics of cells and microcarriers [18]:

$$m_i d\,\overline{v}/dt = F_i = F_{c,i} + F_{b,i} + F_{f,i} + F_{b,i}$$

Where

- m_i is the mass of an agent i representing a microcarrier or a cell.
- $\overline{v}_i$ is velocity of the agent i
- F_i is the total force exerted on agent i
- $F_{c,i}$ is the total force exerted on agent i due to contact with other agents.
- $F_{b,i}$ is the force on cell i due to contact with the bioreactor boundary.
- $F_{f,i}$ is the total force exerted on agent i due to fluid flow, this is the so-called drag force.
- $F_{g,i}$ is the force due to gravity and buoyancy.

The contact force on an agent i is the sum of all mechanical forces that act on agent i due to interactions with other agents and with the bioreactor boundary:

$$F_{c,i} = \sum_{j=1}^{N} F_{ij}$$

where F_{ij} is the force exerted by other agents (cells and microcarriers) that form a bond with agent i. A bond is created between two agents when the distance between their centers becomes smaller than a threshold value δ_c. Similarly, a bond between two agents is broken when the distance between their centers becomes larger than δ_d. The force between bonded agents is treated as a spring-bound system, and is described by the following equations:

$$\delta_{ij} = \alpha R_i + \alpha R_j - d_{ij}$$
$$F_{ij} = K\,\delta_{ij}\,tanh(s_b\,|\delta_{ij}|)$$

where d_{ij} is the distance between the centers of agents i and j. α is a factor applied to cell radii to take into account the volume of the extracellular matrix attached to cells, here we set up the value of α to 1. The bond between two agents, with the parameter K being the spring constant of the bonds, is an attractive force when the distance is greater than $\alpha(R_i + R_j)$ and a repulsive force when the distance is less than $\alpha(R_i + R_j)$. The attractive force between a pair of agents grows with distance until the bond breaks and the agents become unassociated. The stiffness of the bond between two agents is controlled by the parameter s_b. See [19] for a more detailed description of the bond model.

The forces on agents due to contact with the bioreactor boundary is modelled with a repulsive interaction force that is proportional to the overlap $\delta_{b,i}$ between the spherical agent i and the bioreactor boundary:

$$F_{b,i} = -(\varepsilon/\sigma)\, e^{\delta_{b,i}/\sigma}$$

where [20] ε captures the magnitude of the interactions between agents and boundary, and σ is a scale factor of the order of the agents' sizes.

The currently modeled interaction between the fluid and the agents is unilateral: we model the effect of the fluid on each agent, but not, yet, how the flow field is affected by the agents. As the spatial density of agents increases in modeled scenarios, so will the need to model bilateral interactions.

In this work, the fluid drag force is based on Stokes flow past a sphere, and it is given by:

$$F_{f,i} = 6\pi\, \mu\, r_i\, \bar{v}_{r,i}$$

where μ is the dynamic viscosity of the fluid, r_i the radius of agent i, and $\bar{v}_{r,i}$ is the relative velocity of the agent i with respect to fluid velocity [21].

Finally, the effects of gravity and buoyancy on agents are represented by the following equation:

$$F_{g,i} = mg(1 - \rho_m / \rho_i)$$

where g is the standard acceleration of gravity, ρ_m is the density of the medium, and ρ_i is the density of the agent.

5.3.2. Cell growth

To model cell growth, under our current assumption of abundant nutrients, we use the following equations for the biomass of cell i:

$$dm_i/dt = r_{max} \frac{K_S^2}{K_S^2 + \sigma_i^2}$$

m_i : is the biomass of cell

r_{max} : is the maximum proliferation rate obtained directly from the doubling time

σ_i : is the mechanical stress on cell i

K_S : a parameter the modulated the effect of mechanical stress on growth rate

To compute the mechanical stress we first need to compute the tensor stress (S_i) of agent *i*, due to interactions with other agents [22]:

$$S_i = (1/V_i)\left[\tfrac{1}{2}\sum_j F_{ij} \otimes r_{ij}\right]$$

where $\otimes$ is the tensor product of the two vectors, F_{ij} the force and r_{ij} is the distance between agent centers. The volume of the cell (V_i) is computed assuming the cells are of constant density ρ , $V_i = m_i/\rho$. From the volume, we compute the new radii of cells. The mechanical stress used to modulate cell growth is the average of the principal stresses computed as the trace of the stress tensor:

$$\sigma_i = Trace(S_i)/3$$

5.3.3. Cell division

A cell division event is performed when the cell radius is greater than a user defined threshold R_{div} . In cell division, a cell i is replaced by two daughter cells, one daughter has a mass between $(m/2 - 0.1m)$ and $(m/2 + 0.1m)$ (a random value is drawn from a uniform distribution between these two limits) and the other takes the remaining mass to ensure that the total mass is conserved. The two daughter cells are placed in the plane tangential to the microcarrier (sphere) that passes through the center of the mother cell. Only cells that are attached to a microcarrier divide. The direction within the plane in which the two daughter cells are placed is randomly selected. Both daughter cells are placed a distance $(R_1 + R_2)/4$ from the center of the mother cell, where R_1 and R_2 are the radii of the two daughter cells.

Name	Symbol	Value	Source
Cell properties			
Density of cells	ρ_i	8.36e-16 kg/μm^3	[5], [23]
Cell division radius	R_{div}	15 μm	[5], [23]
Maximum radius	R_{max}	16 μm	*
Doubling time	T_d	1.0 s	*
Mechanical stress modulator	K_S	1e-7 μN/μm^2	*
Microcarriers properties			
Microcarrier radius	R_m	150 μm	[24]

Microcarrier density	ρ_m	8.32e-17 kg/μm^3	[24]
Fluid (water) properties			
Density	ρ	1.0e-18 kg/μm^3	
Viscosity	μ	1.0e-9 μN*s/μm^2	
Bioreactor geometry			
Bioreactor height	H_B	42895 μm	[8]
Bioreactor diameter	D_B	55000 μm	[8]
Impeller length	L_I	38000 μm	[8]
Impeller diameter	D_I	8000 μm	[8]
Cell-cell mechanical interactions			
Cell scaling factor (EPS)	α	1.0	*
Cell-cell spring constant	K_{cc}	1e-3 μN/μm	*
Cell-cell bond flexibility	s_{cc}	0.2	*
Thresholding factor for cell-cell bond creation	$f_{c,c}$	1.0	*
Thresholding factor for cell-cell bond breaking	$f_{d,c}$	1.1	*
Cell attachment to microcarriers			
Cell-microcarrier spring constant	K_{cm}	2.2e-3 μN/μm	*
Cell-microcarrier bond flexibility	s_{cm}	0.2	*
Thresholding factor for cell-microcarrier bond creation	$f_{c,m}$	1.0	*
Thresholding factor for cell-microcarrier bond breaking	$f_{d,m}$	1.1	*
Cell bioreactor interactions			
Magnitude of boundary repulsive forces	ε	2.0e-9 μN	*

Scale factor for repulsive forces	σ	1.0	*
Initial conditions for simulations			
Number of microcarriers		~500	*
Number of cells per microcarrier		10	*
Cell radius		[11 - 14.5]	*

Table 1: Parameters of the model. The * symbols indicates that the parameter was manually calibrated.

5.4. Integration

5.4.1. Challenges

Synchronizing CFD and ABM simulations presents unique challenges given the range of the spatial and temporal scales at which modeled behaviors manifest, often orders of magnitude or more apart. Specifically, the time-scale at which eddies form in fluid-flow is on the order of milliseconds whereas the time-scale at which cells divide is many hours; individual cells are hundreths of a millimeter in diameter, whereas bioreactor diameters are anywhere from centimeters to meters in scale. Coupling these techniques can also be computationally demanding and researchers may have to trade off the fidelity of the model against the expense of computation when implementing these two methods in concert [15].

We intend to take on this multiscale challenge as future work. In the current proof-of-concept, we contain the computational expense by simulating cells proliferating on roughly 500 microcarriers in a small bioreactor for just a few minutes of real-time, accelerating the modeled proliferation rate of cells to divide in seconds instead of days. While the quantity of cells is greatly overestimated, the relative growth rate of those quantities at different rotor speeds are comparable. We expect these results to be consistent with simulations of realistic biological time scales, requiring considerably larger computing resources.

5.4.2. Pipeline

The current integration of CFD with ABM takes the form of a pipeline, illustrated in Figure 4. COMSOL computes a fluid velocity field that depends upon the bioreactor geometry as well as input parameters such as the rod's rotational speed and the media's viscosity. The output of the CFD stage is a text file containing a list of points, with each point represented by its three-dimensional coordinates and followed by a corresponding flow velocity.

From these points, a utility routine currently using the CGAL template library computes a tetrahedral mesh data structure supporting fast location of the tetrahedral vertices containing a given point. The ABM model invokes this utility to locate the tetrahedron containing the center of

each cell and microcarrier. The velocity at each center is estimated by interpolating the four velocities corresponding to the tetrahedra vertices. Biocellion, an agent-based high-performance computing software platform for modeling and simulating living systems at cell-resolution, uses these fluid velocities to determine the forces acting on each agent as described earlier. From the forces, Biocellion computes positions of and stress endured by each cell and outputs this data into files periodically during simulation.

Another utility translates this data into a format read-in by a visualization application written in Unity3D. At the time of writing this report, a demo of that application is accessible at thecmmc.org/stirred-tank-demo. The implementation can be found at github.com/TheCMMC in the repositories indicated in Figure 4.

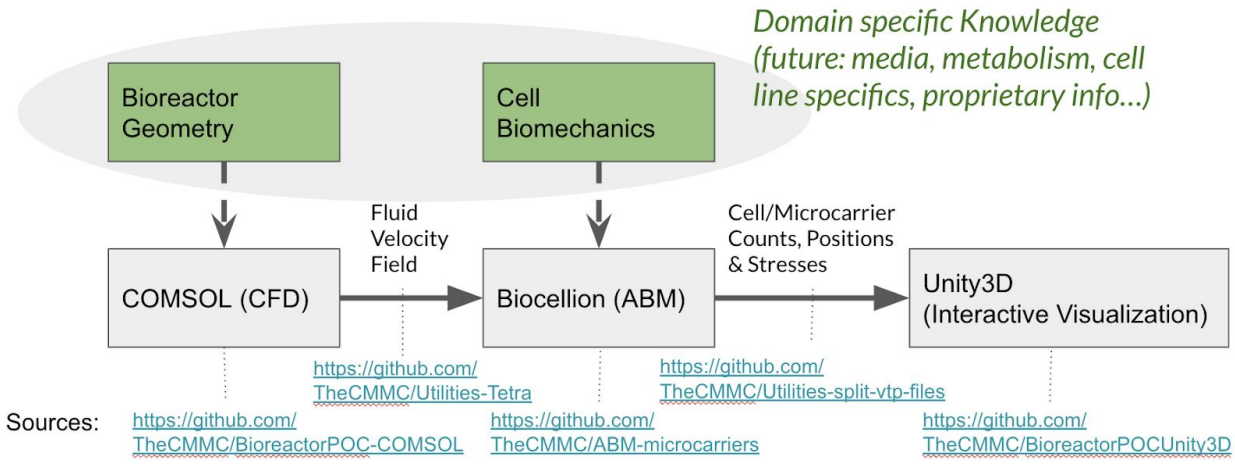

Figure 4. Pipeline architecture of the current modeling methodology.

6. Results

6.1. Flow dynamics: 60 RPM vs 240 RPM

The steady-state flow behaviors (velocity magnitude, shear stress, and Kolmogorov length) at impeller rotation speeds of 60 and 240 rpm are illustrated in Figure 5. These modest rotational speeds induce qualitatively similar flows. One can see from the vertical slice cut parallel to the x-z plane that at both rotor speeds the velocity magnitude is largest near the tips of the impeller and lowest in a vertical cylindrical region at the center. However, as evidenced by the relative ranges on the color-coded legends, the velocity magnitude at 240 rpm is about four to five times that at 60 rpm.

The shear stress and Kolmogorov length are two parameters, also displayed in Figure 4, that influence the biological processes in bioreactors. Similar to the velocity magnitude profiles, the shear stress and Kolmogorov length show similar patterns at 60 and 240 rpm. Generally, a higher shear stress and lower Kolmogorov length exerts more influence on the cells. Higher shear stress and lower Kolmogorov length are observed around the tips of the impellers,

indicating more potential detachment of cells from microcarriers in these regions compared to other regions in the same bioreactor. Unsurprisingly, at 240 rpm shear stress is larger and Kolmogorov length lower than at 60 rpm throughout the bioreactor.

	60 RPM	240 RPM
Velocity magnitude, m/s	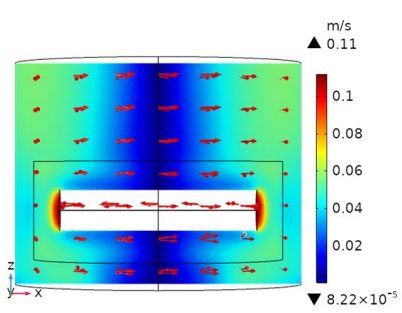	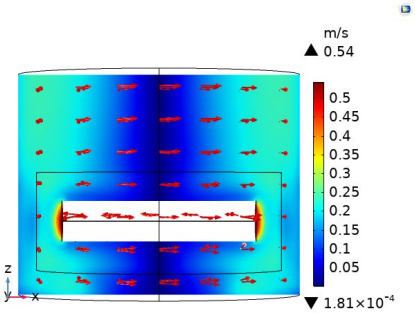
Shear stress, Pa	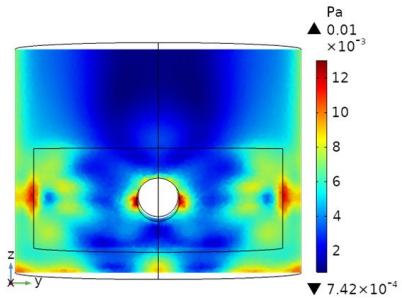	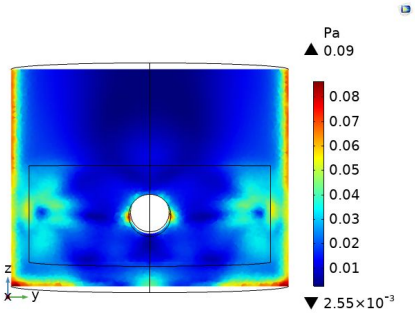
Kolmogorov length, m	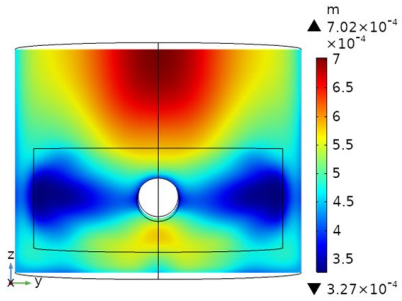	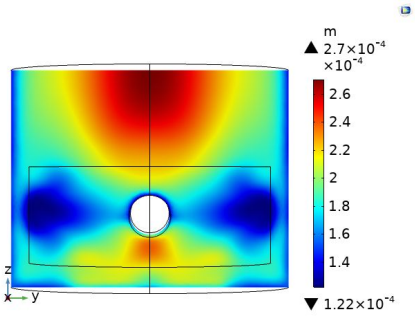

Figure 5. Computational fluid dynamic simulations at 60RPM and 240RPM.

6.2. ABM model of proliferation on microcarrier under zero flow conditions

Using the ABM model described in subsection 5.3, we have simulated cells growing and proliferating on a microcarrier under ideal conditions of zero-flow and abundant nutrients. These baseline simulations enable us to calibrate parameters while ensuring modeled cells behave as expected in a microenvironment composed of neighboring cells on a microcarrier that supports them as they grow. The parameters of the simulations are shown in Table 1. Figure 6B shows a histogram of mechanical stress experienced by cells. For each cell *i*, stress σ_i is computed from the equation in section 5.3.2. Compressive forces contribute positively and expansive forces contribute negatively to the overall mechanical stress sensed by cells. Figure 6A shows a simulation snapshot of cells growing on a microcarrier. The color of cell *i* represents the magnitude of mechanical stress. Most of the cells in this example experience compressive forces exerted by their neighbors as indicated by their reddish color (6A) and by the predominantly positive values for net stress on a cell reported in the histogram (6B). This figure suggests the mechanical stress sensed by the cells on the microcarrier may be highly variable.

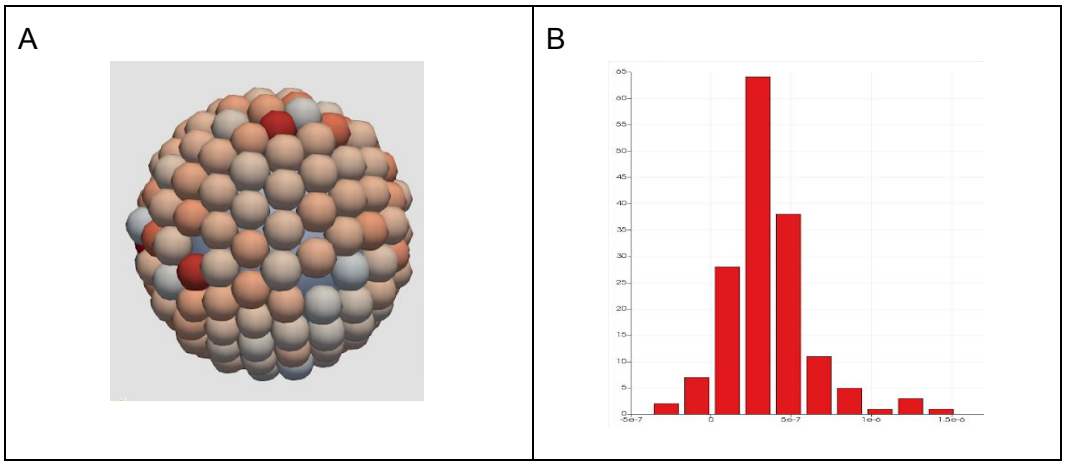

Figure 6. Agent based model of cells on a microcarrier.
(A) Cells growing on top of a microcarrier. Red indicates compressive stress and blue indicates tensile stress. (B) Histogram of mechanical stress sensed by the cells growing on the microcarrier.

6.3. Integrated result

We combined the ABM and CFD methods to create a “whole-system” bioreactor model. In our new model, fluid flow influences how individual cells move, grow and proliferate. Because we had observed in CFD simulations that our modeled bioreactor reaches its steady-state flow in just a few seconds, we ignore transient flows in our whole-system simulation. Also, for the sake of being able to connect mechanics directly to observed effects, we chose not to incorporate at

this stage the Kolmogorov lengths reported by the CFD simulation. As described in Section 5.3.1, we use only the distribution of fluid velocities to compute the drag forces $F_{f,i}$.

Figure 7 shows a simulation snapshot of microcarriers (blue) moving in the bioreactor, following the fluid as they collide with other microcarriers or the bioreactor boundaries. Those boundaries, the vertical red lines, are an artifact of having approximated the circular cylindrical bioreactor as a polygonal cylinder.

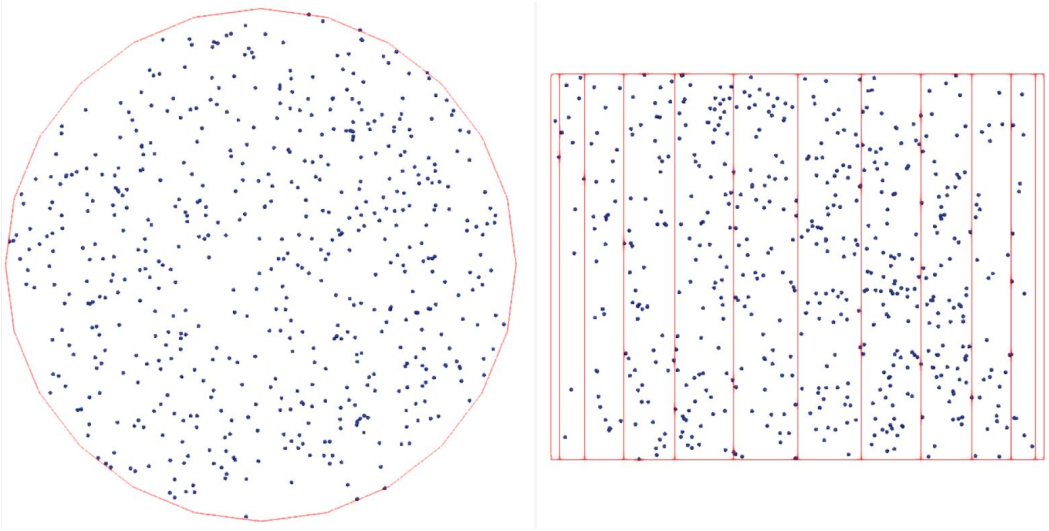

Figure 7. Top (left) and side (right) view of microcarriers moving in the bioreactor.

Figure 8 shows how the number of cells change during the simulations for different values of K_S, a parameter that modulates the effect of mechanical stress on cell proliferation. For $K_S = 1$, the cell count follows exponential growth. For $K_S = 1e-6$ and $K_S = 1e-7$, growth begins along a similar exponential path but eventually deviates, slowing down. For $K_S = 1e-8$ the growth is much slower from the get-go compared to at $K_S = 1$. These results demonstrate that the method can model the effect of mechanical interactions and stresses on proliferation.

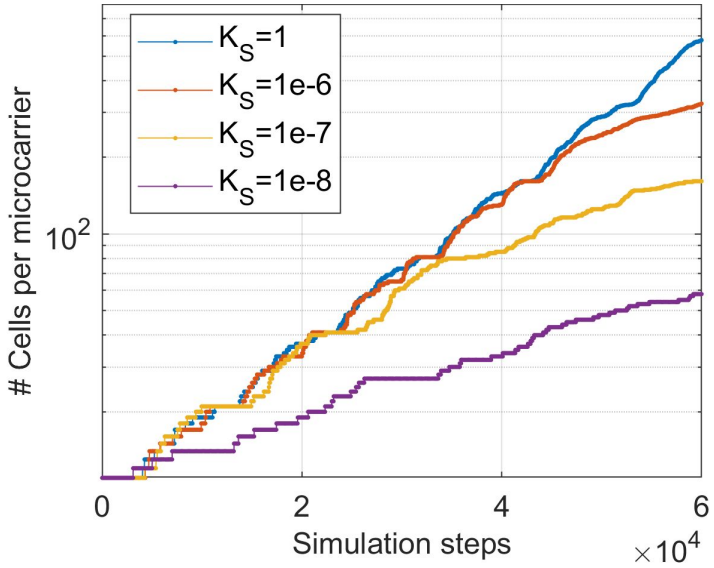

Figure 8. Cell number per microcarrier as a function simulation steps.

We also compared growth rates for whole-system simulations at both 60RPM and 240RPMs. These simulations test whether the model can recapitulate the trends observed experimentally by Croughan *et al,* described in section 4 of this paper. Croughan *et al.* observed that the growth rate of cells in the bioreactor decreases with increasing impeller rotation rate. Figure 9 shows how the number of cells changes in the simulations at 60RPM and 240RPM. These simulation results also show cell count rate decreases with increasing impeller velocity and are in good qualitative agreement with those reported by Croughan *et al*.

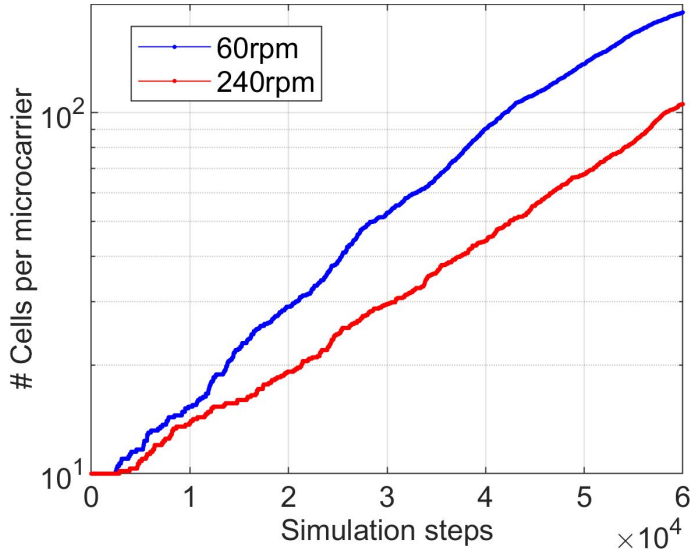

Figure 9 Cell number per microcarrier as a function simulation steps, for different revolution rates of the impeller.

7. Discussion

We have demonstrated, at a proof-of-concept level, that whole-system bioreactor models integrating ABM and CFD can capture the impact of fluid flow on cell behavior, namely, proliferation. We expect to be able to incorporate other cell behaviors and states, such as apoptosis or attachment and spreading of the cell through integrins and focal adhesion molecules, into this framework in a straightforward manner. Our multiscale model recapitulated two previously reported trends observed of cells growing on microcarriers suspended in a stirred tank bioreactor: that at a higher rotor speed (rpm), total biomass production and production rate drop; and that production rate decelerates further as microcarriers saturate.

It is worth reiterating that the present work is preliminary and aims to recapitulate only qualitatively the empirical and theoretical results in Croughan *et al.* [8] while prototyping a new computer modeling methodology. We made several assumptions and simplifications in the model:

I. Assumption. The only impact of mechanical stress on cell biology is to slow cell proliferation rate.
II. Assumption. Capturing the relevant fluid dynamics behaviors is accomplished at a much shorter simulation time-step than is needed to capture the biological response behaviors of cells.
III. Simplification. Biomass growth and microcarrier count does not significantly affect the fluid properties.
IV. Simplification. Cell growth is independent of the concentration of molecules (such as nutrients, oxygen, or H+ ions) in the media.
V. Simplification. Microcarrier and cell densities are less, and proliferation rates greater, than those used and observed in laboratory experiments.

In accordance with assumption I, cells do not die in our model. Notably, previous theoretical studies, specifically Croughan et al. [8], assert that cell death is the main driver of biomass reduction at higher rotor speeds but without providing experimental validation. Our understanding from experimentalists is that dead cells are difficult to count accurately because they may disintegrate into the surrounding media during the experimental period evading measurement post-experiment. Assumption I is tantamount to an alternative hypothesis that the negative impact of mechanical stresses on some cells' proliferation rates alone is responsible for the overall reduced biomass growth rate observed at higher rotor speeds. This hypothesis is supported by our simulations (Figure 9). The ABM approach, facilitating representation of individual cells and the induced mechanical stresses they experience, thus provides a direct means to answer the question: "Instead of cell death, could a reduction in proliferation rate caused by shear and compression stresses on some cells explain the reduced biomass at higher stir speeds?" Answered in the affirmative for virtual experiments, there is now a stronger case for asking the same question of laboratory experimentalists.

Assumption II and Simplifications III and IV simplify integration of ABM and CFD in this early modeling approach. Simplification III implies fluid properties are independent of the cell and microcarrier population. A CFD simulation performed on a bioreactor with only media therefore suffices to predict fluid velocities. Simplification V means both that cell ingest and secretion rates as well as mixing are irrelevant, so that simulation can be performed on a homogeneous fluid. Because steady state is reached in under ten seconds of bioreactor operation, Assumption II permits a steady-state fluid flow to be used at all biological time-steps.

One advantage of this approach is that fluid dynamics can be modeled independently of the cell behavior (Figure 4) as a stage whose output becomes an input to the ABM simulation. There is not yet a need for a feedback edge that would require recomputing CFD. However, all four of these simplifying assumptions are insufficient to bridge the discrepancy in biomechanics and biological time-scales. Namely, that a cell can move from one end of the bioreactor to the other in seconds, whereas its division into two cells takes about a day. Furthermore, simulating the millions of microcarriers and billions of cells in even small bioreactors, while possible using supercomputers, is beyond the computational capability of the desktop computers and small cloud clusters we have readily available. The workaround is Simplification V, to perform simulation using unrealistic proliferation rates in the time scale of seconds, and to use a number of microcarriers considerably smaller than typically used in experiments. The qualitative trends observed in Figures 8 and 9 are not expected to change due to these simplifications. Further model refinements will be needed to model the whole bioreactor system at realistic temporal and spatial time scales.

In spite of the assumptions and simplifications, this unified CFD and ABM model promises to offer an enhanced understanding of microcarrier-based stirred tank bioreactors that was not possible with the analysis conducted by Croughan *et al*. [8]. The damaging effects due to formation of turbulence are of special interest. Researchers investigating turbulence have noticed eddy size determines its effect on solid particles [25]–[27]. Their observations suggest that microcarriers are harmlessly swept away by eddies whose curvature is shallower than the radius of the microcarrier, but that eddies adjacent to a microcarrier of sharper curvature instead exert distortional forces. The eddy-length model specifically proposes that damage occurs to cells when the Kolmogorov eddy length is below a critical value [8]. Given the single cell size spatial resolution that is possible with ABM and the turbulence modeling capability of CFD, this novel computer modeling methodology should make it possible to assess the validity of the eddy-length model theory. Croughan *et al*. [8] also noted that fluctuating fluid velocity components around a microcarrier change rapidly with time and position as it moves throughout a stirred bioreactor. These authors propose a “time-average” analysis model, where the position-dependent time-average flow profile around a microcarrier is tracked as it circulates through various time averaged velocity fields in a stirred tank. Realistically, this is an oversimplification of dynamics within the bioreactor environment, and neglects to capture how this fluid flow variability will manifest across a cell population. Here, the combined CFD-ABM model could offer more detailed information.

8. Future Work

The computer model methodology introduced in this work is the first step towards a more comprehensive model that, in combination with experimental observations, will enable a rational optimization of biomass growth in bioreactors. We identified the following refinements and advancements that will be implemented in a second stage of the model development.

- **Refine the integration of CFD and ABM methods**. In this work the fluid dynamics is assumed to be in a steady state and is thus unaffected by the growing biomass. In the next phase, we aim to model the complete dynamics (including transient behaviour) of the fluid as well as the potential effects of cell growth on fluid dynamics. This refinement will enable the simulation of more realistic experimental scenarios and should facilitate process optimization around modifying the rotor speed to improve mixing and potentially bead to bead transfer of cells.
- **Include viability of cells in the modeling method**. We aim to include cell death induced by mechanical stresses in the cellular microenvironment and by lack of nutrients and oxygen. This refinement is necessary for a validation of the model with experimentally observed trends.
- **Validate model against experimental observations.** For a model to be considered as a valid and predictive representation of a process, the results obtained from the model need to be statistically compared with experimental observations. We aim to identify an industrial partner that can perform experiments focusing on the effect of fluid dynamics on the viability of cells growing on microcarriers and other relevant phenomena in similar stirred-tank bioreactor systems.
- **Improve the computational efficiency of the model at scale**. In order to validate the model simulations with experimental data, it is necessary for the model to be able to perform simulations representing realistic time and spatial scales, and cell densities. We aim to apply statistical and other approaches from the multiscale modeling field to create models at longer and larger scales and for higher populations [28]–[30], [12], [16], [15]. All such approaches rely on first thoroughly vetting our current cell-scale models to ensure they capture the behaviors upon which outcomes depend. Following validation, we plan to generate voluminous data from diverse simulations using these models, to use that data to inform modeling at a larger scale, to revalidate against experiment, and to repeat this process at ever larger scales.
- **Apply to diverse scenarios.** A strength of the approach is its generality. While this work illustrates its application to FS-4 cells growing on spherical microcarriers in a stirred-tank bioreactor, the methodology is no less applicable to other cell lines either growing in suspension or on microcarriers of other shapes or having different properties, or in rocking, hollow fiber, or continuous flow bioreactors. Future work will include adaptation to study the efficacy of biomass production in these and other scenarios of interest.

9. Call to Action

Modeling and simulation does not follow a straight path from knowledge to accurate prediction. Instead it follows an evolutionary cycle, incorporating knowledge and data extracted from physical experiments to create successive prototype models whose predictions, when compared with experimental results, drive iterative improvement. What accelerates progress in modeling is the availability of laboratory scientists to run experiments, make measurements, and offer hypotheses that account for discrepancies. In return, modeling will facilitate testing those scientific hypotheses and ultimately accelerate engineering of novel or optimized solutions. Our call to action is an invitation to scientists to review our approach, ask questions, provide feedback, and to participate in running the experiments needed to further advance and validate our models as they evolve. Contact us at thecmmc.org to learn more.

10. Supplemental material

	Croughan *et al.*, 1986		
Parameter	**Value**	**Magnitude (units)**	**Source**
Cell name	FS-4		1
Cell origin	Human diploid fibroblast		1
Cell shape	-		
Cell diameter	18-22	um	2
Cell volume	3000-6000	um^3	2
Cell mass	3.50E-09	g/cell	3
Microcarrier type	Cytodex-1		
Microcarrier diameter	180	um	4
# microcarriers/mass	6.80E+06	microcarriers/g dry weight	4
Swelling index	18	mL/g dry weight	4
Use density	3	g/L	4
Total # of microcarriers (in 100 mL)	2.04E+06	microcarriers	*
Microcarrier dry mass	1.47E-07	g/dry carrier	*

Microcarrier wet mass	2.79E-06	g/wet carrier	*
Growth temperature (GT)	37	degrees C	1
pH	7.3	-	1
Vessel geometry	5.5	cm (internal diameter)	1
Media volume	100	mL	1
Specific density (@ GT)	1.01	-	1
Density (@ GT)	1.003233	g/cm^3	*
Media viscosity (@ GT) (Newtownian)	1	cP	1
Media height	4.21	cm	*
1/3 media height	1.4	cm	*
Stir bar length	3.8	cm	1
Stir bar diameter	0.8	cm	1
Agitation	60,140,180,220	rpm	1
Medium change (75 %)	4th	day	1
Starting glucose concentration	4.5	g/L	1

Table S1: Table of parameters obtained from [8].

Sources

1. Croughan, M.S., Hamel, J.F., and Wang, D.I. (1987). Hydrodynamic effects on animal cells grown in microcarrier cultures. Biotechnol Bioeng 29, 130-141.

2. https://books.google.ca/books?id=m07VDwAAQBAJ&pg=PT225&lpg=PT225&dq=FS-4+cells+diameter&source=bl&ots=eF_LPLS1U9&sig=ACfU3U2_co9cg1j1UeHyvO0PH3yvO924aQ&hl=en&sa=X&ved=2ahUKEwi_0-fct-_oAhU9hXIEHVFhAS4Q6AEwBHoECAwQNg#v=onepage&q=FS-4%20cells%20diameter&f=false
3. Allan, S.J., De Bank, P.A., and Ellis, M.J. (2019). Bioprocess Design Considerations for Cultured Meat Production With a Focus on the Expansion Bioreactor. Frontiers in Sustainable Food Systems 3.
4. http://www.gelifesciences.co.kr/wp-content/uploads/2016/07/023.8_Microcarrier-Cell-Culture.pdf

*calculated

11. References

[1] P. M. Doran, *Bioprocess Engineering Principles, Second Edi*. Elsevier Ltd, 2013.

[2] A. Grünberger *et al.*, “A disposable picolitre bioreactor for cultivation and investigation of industrially relevant bacteria on the single cell level,” *Lab. Chip*, vol. 12, no. 11, pp. 2060–2068, 2012.

[3] H.-P. Meyer, W. Minas, and D. Schmidhalter, “Industrial-scale fermentation,” *Ind. Biotechnol. Prod. Process.*, pp. 1–53, 2017.

[4] M. Stephenson and W. Grayson, “Recent advances in bioreactors for cell-based therapies,” *F1000Research*, vol. 7, 2018.

[5] S. J. Allan, P. A. De Bank, and M. J. Ellis, “Bioprocess Design Considerations for Cultured Meat Production With a Focus on the Expansion Bioreactor,” *Front. Sustain. Food Syst.*, vol. 3, 2019, doi: 10.3389/fsufs.2019.00044.

[6] S. Kahan, J. Camphuijsen, C. Cannistra, G. Potter, Z. Consenza, and I. Shmulevich, “Cultivated Meat Modeling Consortium: Inaugural Meeting Whitepaper.” Authorea, Inc., doi: 10.22541/au.158057683.31004563.

[7] C. Schirmer, T. Nussbaumer, R. Schöb, R. Pörtner, R. Eibl, and D. Eibl, “Development, engineering and biological characterization of stirred tank bioreactors,” in *Biopharmaceuticals*, IntechOpen, 2018, pp. 87–107.

[8] M. S. Croughan, J.-F. Hamel, and D. I. C. Wang, “Hydrodynamic effects on animal cells grown in microcarrier cultures,” *Biotechnol. Bioeng.*, vol. 29, no. 1, pp. 130–141, 1987, doi: 10.1002/bit.260290117.

[9] C. Zhan, E. Hagrot, L. Brandt, and V. Chotteau, “Study of hydrodynamics in wave bioreactors by computational fluid dynamics reveals a resonance phenomenon,” *Chem. Eng. Sci.*, vol. 193, pp. 53–65, 2019.

[10] “Bioreactor Design Adapts to Biopharma’s Changing Needs,” *GEN - Genetic Engineering and Biotechnology News*, Jul. 01, 2019. https://www.genengnews.com/insights/bioreactor-design-adapts-to-biopharmas-changing-needs/ (accessed Sep. 23, 2020).

[11] J. M. Epstein, R. Pankajakshan, and R. A. Hammond, “Combining Computational Fluid Dynamics and Agent-Based Modeling: A New Approach to Evacuation Planning,” *PLoS ONE*, vol. 6, no. 5, May 2011, doi: 10.1371/journal.pone.0020139.

[12] G. Fullstone, J. Wood, M. Holcombe, and G. Battaglia, “Modelling the Transport of Nanoparticles under Blood Flow using an Agent-based Approach,” *Sci. Rep.*, vol. 5, p. 10649, Jun. 2015, doi: 10.1038/srep10649.

[13] R. Bhui and H. N. Hayenga, “An agent-based model of leukocyte transendothelial migration during atherogenesis,” *PLOS Comput. Biol.*, vol. 13, no. 5, p. e1005523, May 2017, doi: 10.1371/journal.pcbi.1005523.

[14] R. Bhui, “A Multiscale Model of Leukocyte Transendothelial Migration During Atherogenesis,” May 2018, Accessed: Sep. 14, 2020. [Online]. Available: https://utd-ir.tdl.org/handle/10735.1/6583.

[15] A. Corti, C. Chiastra, M. Colombo, M. Garbey, F. Migliavacca, and S. Casarin, “A fully coupled computational fluid dynamics – agent-based model of atherosclerotic plaque development: Multiscale modeling framework and parameter sensitivity analysis,” *Comput. Biol. Med.*, vol. 118, p. 103623, Mar. 2020, doi: 10.1016/j.compbiomed.2020.103623.

[16] M. K. Ozalp *et al.*, “Experiments and Agent Based Models of Zooplankton Movement within

Complex Flow Environments," *Biomim. Basel Switz.*, vol. 5, no. 1, Jan. 2020, doi: 10.3390/biomimetics5010002.
[17] C. A. Peng and B. Ø. Palsson, "Cell growth and differentiation on feeder layers is predicted to be influenced by bioreactor geometry," *Biotechnol. Bioeng.*, vol. 50, no. 5, pp. 479–492, Jun. 1996, doi: 10.1002/(SICI)1097-0290(19960605)50:5<479::AID-BIT2>3.0.CO;2-C.
[18] P. G. Jayathilake *et al.*, "A mechanistic Individual-based Model of microbial communities," *PloS One*, vol. 12, no. 8, p. e0181965, 2017.
[19] B. Aguilar, A. Ghaffarizadeh, C. D. Johnson, G. J. Podgorski, I. Shmulevich, and N. S. Flann, "Cell death as a trigger for morphogenesis," *PloS One*, vol. 13, no. 3, p. e0191089, 2018.
[20] R. Hartmann *et al.*, "Emergence of three-dimensional order and structure in growing biofilms," *Nat. Phys.*, vol. 15, no. 3, pp. 251–256, Mar. 2019, doi: 10.1038/s41567-018-0356-9.
[21] S. H. L. Kriebitzsch, M. A. van der Hoef, and J. a. M. Kuipers, "Drag force in discrete particle models—Continuum scale or single particle scale?," *AIChE J.*, vol. 59, no. 1, pp. 316–324, 2013, doi: 10.1002/aic.13804.
[22] A. T. Fenley, H. S. Muddana, and M. K. Gilson, "Calculation and Visualization of Atomistic Mechanical Stresses in Nanomaterials and Biomolecules," *PLoS ONE*, vol. 9, no. 12, p. e113119, Dec. 2014, doi: 10.1371/journal.pone.0113119.
[23] W.-S. Hu, *Cell culture bioprocess engineering*. CRC Press, 2020.
[24] "Microcarrier Cell Culture Principles and Methods." [Online]. Available: http://www.gelifesciences.co.kr/wp-content/uploads/2016/07/023.8_Microcarrier-Cell-Culture.pdf.
[25] R. Kuboi, I. Komasawa, and T. Otake, "Fluid and particle motion in turbulent dispersion—II: Influence of turbulence of liquid on the motion of suspended particles," *Chem. Eng. Sci.*, vol. 29, no. 3, pp. 651–657, 1974.
[26] A. M. Petenate and C. E. Glatz, "Isoelectric precipitation of soy protein. II. Kinetics of protein aggregate growth and breakage," *Biotechnol. Bioeng.*, vol. 25, no. 12, pp. 3059–3078, 1983.
[27] L. A. Glasgow and R. H. Luecke, "Mechanisms of deaggregation for clay-polymer flocs in turbulent systems," *Ind. Eng. Chem. Fundam.*, vol. 19, no. 2, pp. 148–156, 1980.
[28] A. Lapin, J. Schmid, and M. Reuss, "Modeling the dynamics of E. coli populations in the three-dimensional turbulent field of a stirred-tank bioreactor—A structured–segregated approach," *Chem. Eng. Sci.*, vol. 61, no. 14, pp. 4783–4797, Jul. 2006, doi: 10.1016/j.ces.2006.03.003.
[29] J. Zieringer and R. Takors, "In Silico Prediction of Large-Scale Microbial Production Performance: Constraints for Getting Proper Data-Driven Models," *Comput. Struct. Biotechnol. J.*, vol. 16, pp. 246–256, 2018, doi: 10.1016/j.csbj.2018.06.002.
[30] A. Corti, S. Casarin, C. Chiastra, M. Colombo, F. Migliavacca, and M. Garbey, "A Multiscale Model of Atherosclerotic Plaque Development: Toward a Coupling Between an Agent-Based Model and CFD Simulations," in *Computational Science – ICCS 2019*, Cham, 2019, pp. 410–423, doi: 10.1007/978-3-030-22747-0_31.